

# Uncertainty Analysis of Data Collected Using Embedded Magnetic Particle Velocity Gauges

S.G. Finnegan<sup>1,2(a)</sup>, G.J. Appleby-Thomas<sup>1</sup>, R. Hazael<sup>1</sup>, J.W. Ferguson<sup>2</sup>, M.J. Goff<sup>2</sup>

<sup>1</sup>*Cranfield University, Cranfield Defence and Security, Shrivenham, United Kingdom, SN6 8LA*

<sup>2</sup>*AWE, Aldermaston, Reading, United Kingdom, RG7 4PR*

<sup>a)</sup> *S.G.Finnegan: simon.g.finnegan@cranfield.ac.uk*

**Abstract.** The uncertainties in particle velocity and position-time data collected using embedded magnetic gauges are presented. Data were also collected on the resistance change of gauge elements under shock loading and the effect of the element width, as opposed to length, on the observed rise times, as two factors that can affect the data quality and uncertainty analysis. A new method of fitting to the shock tracker data is also proposed. The data were collected using gas gun experiments on Comp-B and PCTFE targets. For a well characterized setup, the uncertainty in the particle velocity data can be reduced to such a level that noise and other ‘random’ variations in the data can be more significant. This highlights the importance of reducing these factors and collecting high quality data but also investigating additional sources of error, such as the resistance change of the elements under shock loading, in order to determine the true uncertainty.

## INTRODUCTION

Embedded magnetic particle velocity gauges are used to record the propagation of a one-dimensional shock or detonation wave through an explosive, and the particle velocity histories at different points within the explosive [1]. Current gauge packages tend to consist of multiple individual elements that are embedded at an angle within a target so that each is located at a different depth. Each element moves at the local particle velocity behind the shock wave and, as the target is sat within a magnetic field, generates a voltage proportional to the velocity, magnetic field strength and length of each element. The gauge packages also typically include ladder elements that generate a stepped signal as the shock moves across them. These elements, known as shock trackers, are used to record position-time data at a higher resolution than the particle velocity elements and determine the point of turnover to detonation in shock to detonation experiments. More details of the design and operating principles of gauge can be found in the literature [1].

In this paper, the magnitudes of the uncertainties in the two types of data are discussed, and data on the resistance change of a gauge element under shock loading and the effect of element dimensions on the rise time, and so resolution, of the diagnostic are presented, alongside a new proposed method of fitting to shock tracker data.

## UNCERTAINTY ANALYSIS OF PARTICLE VELOCITY DATA

Particle velocity,  $u_p$ , data is derived from the measured voltage at the oscilloscope using equation 1.

$$u_p = \frac{V_{scope}}{\left(\frac{-dB}{10^{20}}\right)BL} \frac{R+R_T}{R_T} \quad (1)$$

Where  $V$  is the measured voltage,  $R$  is the gauge element resistance,  $R_T$  the digitizer channel resistance,  $B$  the magnetic field strength,  $L$  the length of the gauge and  $dB$  the value of an attenuator used to protect the digitizer channel from an over voltage. Each of these variables can be characterized leading to a total uncertainty in the data of approximately 4%, with the largest source of the error being the attenuator uncertainty. Without the attenuators the uncertainty is approximately 1%. An example data set from a Comp-B experiment is shown in fig. 1. The experiment

used a cover disk to embed the first gauge element at  $\sim 6$  mm into the target, hence the reaction evident behind the first element. The uncertainties are shown as shaded regions on each trace.

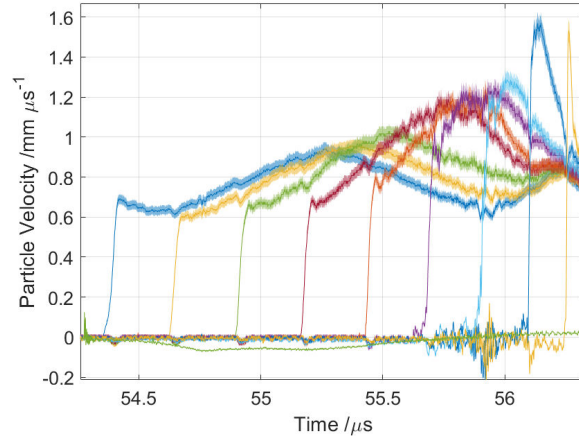


**FIGURE 1:** Particle velocity data with shaded bands displaying uncertainty

As can be seen in fig. 1, the uncertainty is smaller than the random variation in the signal that will arise from electrical noise, glue layers [10] and crosstalk. Therefore, it is important to reduce these features while collecting high quality data. The uncertainty quoted is derived from the measured uncertainties in equation 1 and the digitizer resolution, but this assumes that the resistance of the gauge elements is held constant. If the resistance changes, then the uncertainty would have to increase.

### Resistance Change During Shock Loading

Resistance changes have been observed in the literature for thin metal foils of comparable dimensions to PV gauge elements [4,5] and the phenomena has even been used to measure the temperature behind a shock wave [6]. Since the resistance of the gauge is used to convert the recorded voltage to  $u_p$  data then it is important to characterize any potential resistance changes. A single shot was performed using a constant current power supply, usually used with manganin stress gauges, connected to the elements within a PV gauge without a magnetic field. The data for the first three elements is shown in fig. 2(a). The data is corrected as in [7] since a copper flyer was fired at  $802 \text{ ms}^{-1}$ , generating a pressure of  $\sim 4.5$  GPa within the PCTFE target. The gauge design was supplied by AWE and uses printed silver elements. Unlike manganin, the silver does not have a constant resistance with temperature and so there was an observed resistive heating effect in the baseline of the data, though this is not significant compared to the change at the shock arrival. This 2-3% change is most likely a piezoresistive effect from the shock compression. The data is shown as a percentage resistance change in the gauge in fig. 2(a). The error arising from using the original resistance value rather than the changing resistance value when converting the data to particle velocity is shown in fig. 2(b).

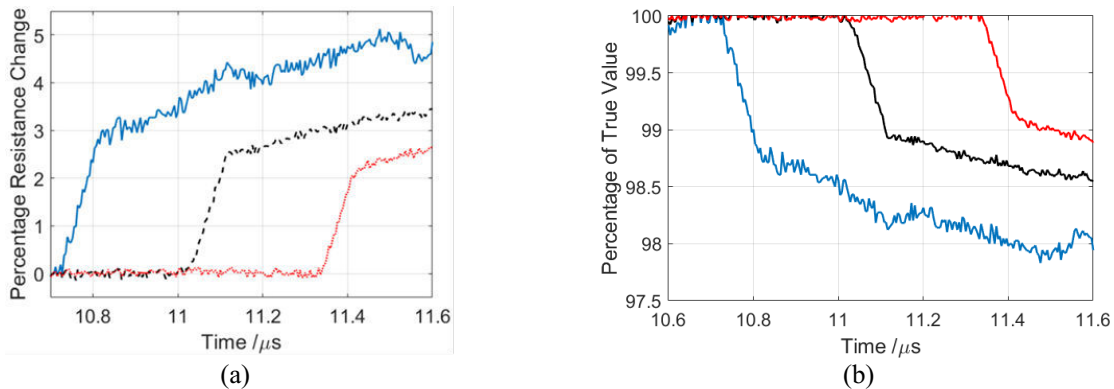


**FIGURE 2:** (a) Percentage resistance change for the first three elements within a gauge package and (b) the effect of using the original resistance value on the conversion of the voltage recorded at the oscilloscope to particle velocity.

Figure 2(b) shows the error arising from the change of resistance at the shock front to be significant compared to the other sources of uncertainty. There is also a rise in resistance beyond the shock that is large. The cause of this is not known though it could be increased resistive heating through the shocked and compressed gauge or possibly a heating of the gauge by the shocked material causing a rise in resistance. The shock loading was a short duration pulse and no evidence of the arrival of the release can be seen in the data, which suggests that the continued rise could be due to resistive heating.

### Remaining Sources of Uncertainty

It is worth drawing attention to other sources of uncertainty discussed in the literature that have not been addressed here. Material slip around the gauge [3], especially during reaction if the viscosity of the material changes, and the effect of an impedance mismatch between the material and the gauge/glue layers resulting in a measured particle velocity different to that in the target material [9, 10] are both topics that should be addressed to completely quantify the uncertainty.

### EFFECT OF GAUGE WIDTH ON RISE TIME

Rise time is known to be dependent upon the time to accelerate the gauge [9] (which is suggested to take multiple reflections across the gauge element and so the gauges are made to be shallow), the oscilloscope response and the tilt of the shock relative to the gauge element. The tilt affects the time taken for the shock to travel the length of the gauge. This therefore implies that the width of the gauge will also determine the rise time observed in the data. To investigate this a simple model was created in which the width and depth of the gauge element are combined into an ‘effective depth’, which represents the distance covered by the gauge along the direction of the shock propagation, when embedded at a known angle. This is illustrated in fig. 3 (a). Using this effective depth value and the length of the gauge element, the gauge can now be considered as a rectangle in which a tilted shock will cross at an angle. The particle velocity value recorded by the gauge was then calculated as the expected shock particle velocity multiplied by the fractional area of the gauge traversed by the shock. Figure 3(b) illustrates how the passage of an angled shock across a gauge element, in red, can be mapped across to a rectangle on the plane of shock motion, in blue.

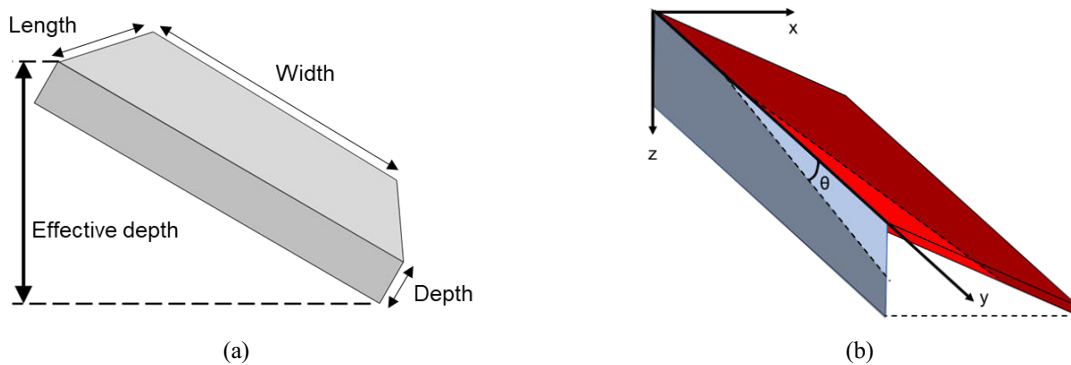


**FIGURE 3:** (a) Cross-sectional diagram of a gauge element to illustrate the quantities defined here as length, width and depth for the angled embedded element, and (b) diagram of how the simple model considers the 3D footprint of the gauge, red, as a 2D rectangle, blue, and how an angled shock would move across it, illustrated by the unshaded regions, moving in the z direction.

This model then creates both a prediction for the rise time, taken as the time to go from 10% to 90% of the maximum particle velocity, and the shape of this rise for different shock velocities and tilt values. It should be remembered that this tilt value will incorporate both dynamic tilt and static misalignment of the gauge to the shock. The model suggested that the width of the gauge has a significant effect on the rise times, and also that some tilt values will cause the signal to show significant rounding in the observed rise. If a tilt angle is such that the shock passes diagonally through the corners of the modelled rectangle, then there will be no linear portion of the rise at all. This could have implications for choosing a particle velocity value for the initial shock in a highly reactive explosive shot as the transition point between the shock rise and subsequent reaction may be less obvious.

A comparison between the model and experimental data collected using a custom gauge shows this rise time dependence upon gauge width to be true. The gauge positioned elements with different widths, but of equal length, at the same depth into a PCTFE target. The resulting data is shown in fig. 4(a), overlaid with predictions from the model with the variables used to generate the model data, which came from the shot conditions. The chosen value of 3 mrad generated data that agreed very well for all three gauge widths considered, which were 150  $\mu\text{m}$ , 500  $\mu\text{m}$  and 1 mm. The effect on the rise time is significant, ranging from  $\sim 40$  to 175 ns for the same shock loading.

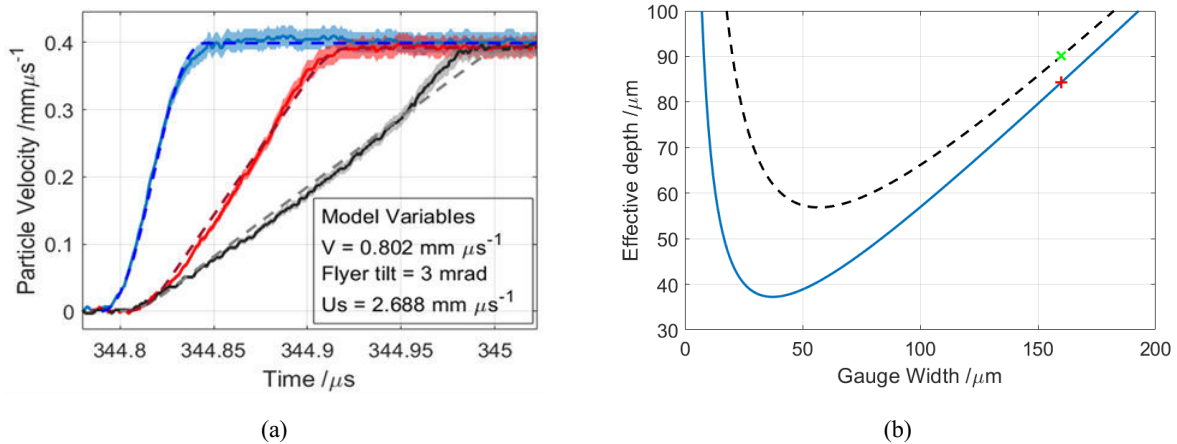


**FIGURE 4:** (a) Experimental data for elements embedded at the same depth within a single experiment but with gauge widths of 150  $\mu\text{m}$  (blue), 500  $\mu\text{m}$  (red), and 1 mm (black), with shaded uncertainties on the  $u_p$  values, alongside model predictions for the same conditions, shown as dashed lines. (b) curves showing the relationship between gauge depth and width for a fixed cross-sectional area. The solid blue line is the true effective depth whereas the dashed black line includes an additional factor of the distance between two sides along the z axis, representing an additional shock reflection. The two highlighted points are the current gauge design.

This may not be a surprising result, but it has possible implications for optimizing gauge designs to minimize the effective depth, since this is a limitation on the minimum rise time. Figure 4(b) shows a relationship between the effective depth and the gauge width, when the cross-sectional area of the element is held constant as an analogue for the resistivity of the element. The dashed black curve has an additional factor representing the distance travelled by a single reflected shock within the element, since the shock may need to ring up within the element. For both curves the current gauge is highlighted as a single data point. Consequently, since the minimum rise time is limited by the width of the gauge, the gauge design can be optimized to improve resolution by reducing the width. However, it will be necessary to balance this with the effect of greater intrusion within the material for a thicker gauge package.

## SHOCK TRACKER DATA

Using a technique of characterizing the gauge in advance and its location as part of the target build, the position of each gauge element can be determined with a total positional uncertainty of approximately 60  $\mu\text{m}$ . For a single shock tracker though, displacing the gauge will move all elements equally and so the relative positional uncertainty between each ladder element is 15-35  $\mu\text{m}$ , when embedded within the target.

It is the relative positional uncertainty that should be used when weighting a fit to the data and the total positional uncertainty when determining the run-to-detonation (RTD) distance or relating the particle velocity data to the shock tracker data.

## Cubic Smoothing Splines

Figure 5(a) shows some example x-t data from three shock trackers embedded within an explosive target. Also shown are the residuals (multiplied by 100) and the relative positional error bars. For comparison the total positional uncertainty is shown as the larger error bars for one set of shock tracker data. The fit to the x-t data was obtained using a cubic smoothing spline function in MATLAB [8]. The proposal for using a cubic smoothing spline is that the functions are continuous over the first and second derivatives, and so can be used to derive velocity and acceleration

relationships, but also that splines could be applied to data from complex shock initiation experiments where acceleration profiles will vary for each loading condition. The exact method of applying the smoothing splines and determining the RTD distance shall be expanded upon in another paper but, for reference, the shock velocity relationship derived from one of the shock trackers is shown in fig. 5(b). The uncertainty analysis was performed in a similar way to [1], using a Monte Carlo approach with the relative positional uncertainties and the uncertainty in locating the center of each rise for the individual shock tracker elements.

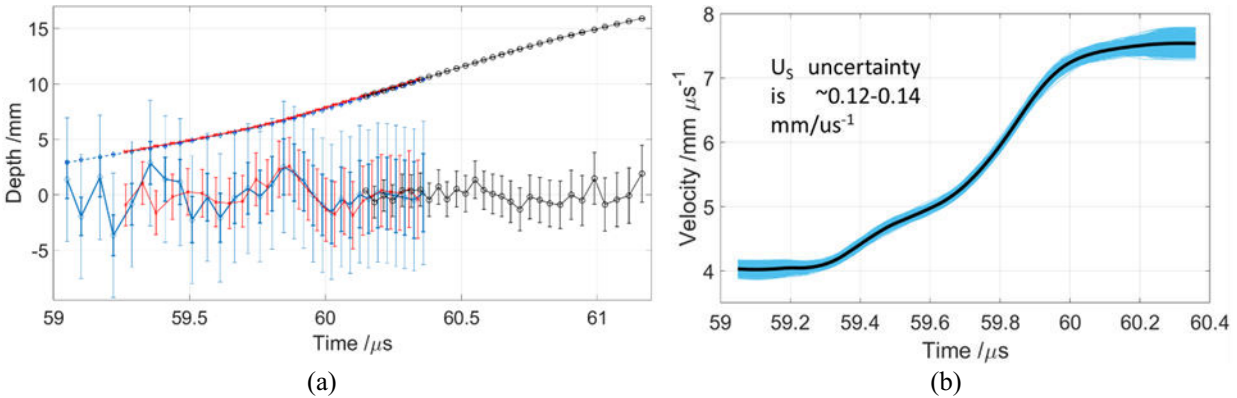


**FIGURE 5:** (a) Shock tracker data for three shock trackers within the same explosive experiment and the residuals multiplied by 100. The residuals also show the total (faint) and relative (bold) uncertainties. The fit was achieved using a cubic smoothing spline [8] and the resulting velocity trace is shown in (b).

## CONCLUSION

The uncertainty in particle velocity data collected by an embedded gauge package, based upon the conversion using equation 1, can be less significant than noise in the data arising from glue layers, electrical noise or cross talk. Therefore, it is important to minimize these additional factors to collect high quality data. Furthermore, for the printed gauges used in these tests, the resistance change observed at the shock front was significant compared to other sources of error. This demonstrates that it is important to quantify this and other sources of uncertainty identified in the literature [3,9,10] such as material slip at the gauge boundaries and the effect of an impedance mismatch between the gauge and the material, in order to fully understand the uncertainty. A new method of cubic smoothing spline fitting has been proposed for use with shock tracker data from complex shock loadings and a dimensional effect on the rise time of the gauge elements has been identified that could lead to optimization of gauge designs to increase the resolution.

UK Ministry of Defence © Crown owned copyright 2022/AWE

## REFERENCES

1. AIP Conference Proceedings 505, 1043 (2000)
2. M.J. Burns, C. Chiquete, J. Appl. Phys. 127, 215107 (2020)
3. J.B. Bdzil, “Fluid Mechanics of an Obliquely Mounted MIV Gauge”, LA-UR-18-22397, 2018
4. V.V. Rodionov, A.I. Goncharov, Combust. Explos. Shock Waves 31, 1–6, (1995)
5. S.D. Gilev, V.S. Prokop’ev, Combust. Explos. Shock Waves 52, 107–116 (2016)
6. D.D. Bloomquist, S.A. Sheffield, AIP Conference Proceedings 78, 304 (1982)
7. M. Goff et al., J. Phys.: Conf. Ser. 500, 142017 (2014)
8. CSAPS, Copyright MATLAB 1987-2010, The MathWorks, Inc.
9. S.J. Jacobs, D.J. Edwards, Fifth Symposium (International) on Detonation, 1970, p. 413
10. R. Menikoff, LA-UR-21-21769, 2021